Ionics (2020) 26:1285–1295
https://doi.org/10.1007/s11581-019-03314-9

ORIGINAL PAPER

Cobalt-free perovskite $Ln_{0.5}Sr_{0.5}Fe_{0.8}Cu_{0.2}O_{3-\delta}$ (Ln = Pr, Nd, Sm, and Gd) as cathode for intermediate-temperature solid oxide fuel cell

Xinmin Fu[1,2] · Minghui Liu[1,2] · Xiangwei Meng[1,3] · Shiquan Lü[1,3] · Danyang Wang[1] · Yihong Zhang[1] · Hongbo Liu[1] · Mingxing Song[2] · Zhiwei Li[3] · Lizhong Wang[2]

Received: 19 July 2019 / Revised: 27 September 2019 / Accepted: 20 October 2019 / Published online: 12 November 2019

Abstract

$Ln_{0.5}Sr_{0.5}Fe_{0.8}Cu_{0.2}O_{3-\delta}$ (LnSFC, Ln = Pr, Nd, Sm, Gd) perovskite oxide as a cobalt-free cathode was systematically evaluated for intermediate-temperature solid oxide fuel cell (IT-SOFC). XRD results show that PrSFC presents the cubic structure, while NdSFC, SmSFC, and GdSFC present an orthorhombic structure. The conductivity of the four samples is in accordance with the GdSFC < SmSFC < NdSFC < PrSFC relationship. AC impedance testing was performed using a symmetrical fuel cell of the structure LnSFC/$Ce_{0.9}Sm_{0.1}O_{1.95}$(SDC)/LnSFC. The polarization resistance values of PrSFC, NdSFC, SmSFC, and GdSFC are 0.036, 0.089, 0.097, and 0.160 Ω cm^2 at 800 °C, respectively. Then, SDC electrolyte-support single cell was fabricated and the power densities of PrSFC, NdSFC, SmSFC, and GdSFC cathodes were 364, 311, 254 and 104 mW cm^{-2}, respectively, at 800 °C. Our preliminary experiment results show that LnSFC oxide meets the requirements of the electrode, and it can be a possible cathode for IT-SOFC.

Keywords Cobalt-free cathode · SOFC · Impedance spectroscopy · Fuel cell performance

Introduction

With the increase of global fossil energy consumption and environmental pollution, exploring new green energy is currently the hottest and most relevant research topic [1–3]. Solid oxide fuel cell (SOFC) is electrochemical device which convert the chemical energy of fuels directly into electrical energy in an efficient and clean way. It has the superiority of fuel efficiency and low environmental pollution [4, 5]. However, the conventional SOFC generally has a relatively high operating temperature (850~1000 °C), which cause various problems such as interfacial reaction, seal hard, and the high cost, resulting in a decrease in performance of SOFC. Therefore, lowering the operating temperature is particularly important. Unfortunately, the reduction in temperature will cause a decrease in cathode catalytic performance. Consequently, it is the primary research direction to find new cathodes with high catalytic performance and low polarization loss in intermediate temperatures (500~800 °C) [6, 7].

In the past, $La_{1-x}Sr_xMnO_{3-\delta}$ (LSM) [8, 9] cathode materials have been extensively studied. However, the ion conductivity of LSM cathode is lower at intermediate temperature. And thus, the polarization resistance becomes large, resulting in a decrease in the electrochemical performance of the cathode. Recently, many cobalt-based perovskite cathodes such as $Ba_{0.5}Sr_{0.5}Co_{1-y}Fe_yO_{3-\delta}$ and $Ln_{1-x}Sr_xCo_{1-y}Fe_yO_{3-\delta}$ (Ln = La, Sm) [10–12] have been well studied. The researchers demonstrate that these cobalt-based cathodes exhibited high ionic and electronic conductivity and excellent catalytic properties. For example, Tu et al. [13] investigated the properties of $Ln_{0.4}Sr_{0.6}Co_{0.8}Fe_{0.2}O_{3-\delta}$ (LnSCF, Ln = La, Pr, Nd, Sm, Gd) cathode materials. They demonstrated that the thermal expansion coefficient (TEC) and electrical conductivity decrease with the Ln^{3+} ion size decreasing from Ln = La to Gd. This indicates that LnSCF oxide such as Gd^{3+} with the smallest ion

✉ Xiangwei Meng
xwmeng2008@126.com

✉ Lizhong Wang
wlz8279@126.com

[1] Key Laboratory of Functional Materials Physics and Chemistry of the Ministry of Education, Jilin Normal University, Siping 136000, People's Republic of China

[2] College of Information Technology, Jilin Normal University, Siping 136000, People's Republic of China

[3] College of Physics, Jilin Normal University, Siping 136000, People's Republic of China

size can effectively reduce TEC. Unfortunately, the TEC of LnSCF for Ln = La to Gd is 21.1–17.6 × 10^{-6} K^{-1}, which is much higher than the commonly used intermediate temperature electrolytes (~ 12 × 10^{-6} K^{-1}). High TEC values limit the use of these Co-based oxides as SOFC cathodes. The instability and high cost of cobalt is another issue. Therefore, developing cobalt-free cathodes with sufficient catalytic activity is significant.

Recently, Fe-based perovskite oxides, $Ln_{1-x}Sr_xFeO_3$ (Ln = La, Pr, Nd, Sm, Eu, and Gd) [14, 15] and $Ba_{1-x}Sr_xFeO_3$ [16–18], have shown good catalytic activity as cathode material. For instance, the polarization resistance (R_p) of $Pr_{0.8}Sr_{0.2}FeO_{3-\delta}$ cathode achieves 0.886 Ω cm^2 at 750 °C. More recently, many researchers reported that partial substitution of Cu by Fe could further improve oxygen mobility for the oxygen reduction reaction (ORR). The R_p of $Bi_{0.5}Sr_{0.5}Fe_{0.8}Cu_{0.2}O_{3-\delta}$ [19], $Pr_{0.6}Sr_{0.4}Cu_{0.2}Fe_{0.8}O_{3-\delta}$ [20], and $BaFe_{0.85}Cu_{0.15}O_{3-\delta}$ [21] cathode materials were 0.13, 0.07, and 0.35 Ω cm^2 at 700 °C, respectively. Moreover, the average TEC of $Pr_{0.6}Sr_{0.4}Cu_{0.2}Fe_{0.8}O_{3-\delta}$ at 50 to 800 °C is 16.4 × 10^{-6} K^{-1}, which is smaller than the TEC of many cobalt-based cathodes [22]. However, there is no report on the systematic study for the $Ln_{0.5}Sr_{0.5}Fe_{0.8}Cu_{0.2}O_{3-\delta}$ (LnSFC, Ln = Pr, Nd, Sm, Gd) oxides until now. In this paper, cobalt-free LnSFC was prepared and investigated as potential applications for the cathode material of IT-SOFCs. The $Ln_{0.5}Sr_{0.5}Fe_{0.8}Cu_{0.2}O_{3-\delta}$ (Ln = Pr, Nd, Sm, and Gd) oxide was synthesized by a sol-gel method, and the effect of lanthanide on electrochemical performance was systematically investigated.

Experimental

Sample synthesis

The powder of $Ln_{0.5}Sr_{0.5}Fe_{0.8}Cu_{0.2}O_{3-\delta}$ (LnSFC, Ln = Pr, Nd, Sm, and Gd) was synthesized by sol-gel method. Pr_2O_3, Nd_2O_3, Sm_2O_3, Gd_2O_3, $Sr(NO_3)_2$, $Fe(NO_3)_3{\cdot}9H_2O$, and $Cu(NO_3)_2{\cdot}3H_2O$ were weighed according to the stoichiometric ratio. Nitrate solutions were prepared by dissolving Pr_2O_3, Nd_2O_3, Sm_2O_3, and Gd_2O_3 in nitric acid, respectively. Other nitrates were dissolved in deionized water. And citric acid (a complexing agent) was added in the mixed nitrate solutions. The ratio of cation to citric acid is 1:1.2. After that, the mixture was placed on a magnetic stirrer, heating and stirring continuously until the solution was viscous, put it in a drying oven at 150 °C for 3 h, removed organics and then grinded it to obtain the precursor powder, and then it was calcined at 950 °C for 10 h. The SDC electrolyte powder was prepared by a glycine combustion method (GNP) [23]. According to the stoichiometric ratio, the corresponding masses of CeO_2 and Sm_2O_3 were weighed and dissolved in concentrated nitric acid to prepare a nitrate solution. The glycine as a complexant was added into the mixed nitrate solution. The mole ratio of total metal ions/glycine is 1:1.2. The above mixed glycine-nitrate solution was heated on a hot plate until the final combustion to obtain an ultrafine powder. The SDC powder was calcined at 600 °C for 6 h. The anode was NiO-SDC (65:35 by weight).

Cell fabrication

The impedance measurement is using a symmetrical cell of the LnSFC|SDC| LnSFC structure. The LnSFC powder was thoroughly mixed with an appropriate amount of organic matter to obtain cathode slurry. LnSFC slurry was screen-printed onto both sides of the SDC electrolyte disk (0.4 mm), and then sintered at 950 °C for 2 h. The power density of LnSFC cathode material was carried out using an electrolyte-supported single cell. First, the anode material was thoroughly mixed with a binder, coated on one side of an SDC pellet with 0.3 mm thickness, and sintered at 1250 °C for 4 h. After that, LnSFC slurry was applied to the other side of SDC pellet and sintered at 950 °C for 2 h in the muffle furnace. Finally, the single cell was sealed with silver paste at one end of the alumina tube. The final valid surface area of the cell was about 0.1 cm^2.

Measurements

An X-ray diffractometer (Rigaku-D-Max γA, Japan) was used to measure the crystal structure of the LnSFC powder. The microstructure of cell cross-section was investigated by a scanning electron microscope (JEOL JSM-6480LV). The valence of the LnSFC material was analyzed using ESCALAB 250XI (Thermo Fisher, USA). The temperature function of the conductivity was measured using a standard dc four-terminal method. The electrochemical impedance spectrum was measured by a CHI660C workstation with 0.01~100 kHz frequency range under open-circuit conditions. The single cells with the NiO + SDC|SDC|LnSFC structure were tested at a temperature of 600~800 °C. The cathode gas is air and the anode gas is H_2.

Results and discussion

Phase structures

The XRD patterns of LnSFC powders calcined at 950 °C for 10 h are displayed in Fig. 1a. These samples exhibited a single-phase structure consistent with previously reported results [24–26]. The PrSFC material presents a cubic perovskite structure and the space group is *pm-3m*. However, the NdSFC, SmSFC, and GdSFC materials exhibit an orthogonal structure with space group *pnma*. The average ion radius of A-site

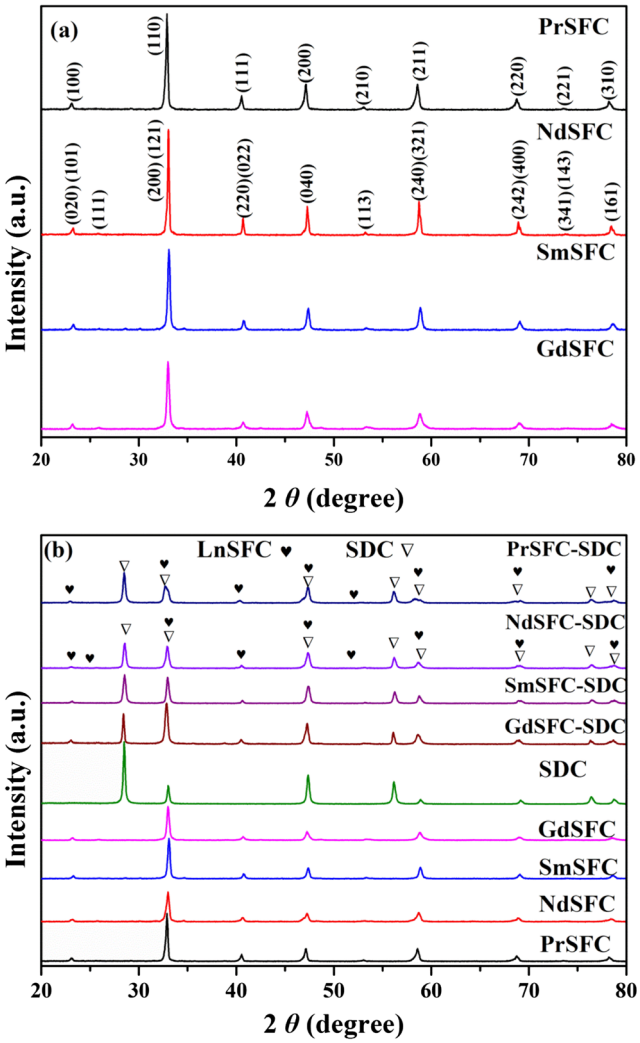

Fig. 1 **a** XRD patterns of the as-synthesized $Ln_{0.5}Sr_{0.5}Fe_{0.8}Cu_{0.2}O_{3-\delta}$ powders. **b** LnSFC-GDC mixture sintered at 950 °C for 2 h

cation is reduced with the radius of the lanthanide cation decreasing from Pr to Gd. This presumably may be the reason why the crystal structure changes from a cubic structure to an orthorhombic structure [27, 28]. The structure parameter is shown in Table 1. The orthorhombic lattice constant decreases as the ionic radius decreases, and a similar phenomenon is observed in other perovskite oxides [29]. Figure 1b shows the XRD patterns of the mixtures of LnSFC cathode and SDC electrolyte. The LnSFC powder was sintered with SDC (50:50 wt.%) at 950 °C for 10 h. It can be seen that no additional peaks appear, indicating that SDC can act as an electrolyte material for the LnSFC cathode.

Table 1 Lattice parameters of the $Ln_{0.5}Sr_{0.5}Fe_{0.8}Cu_{0.2}O_{3-\delta}$ samples

Samples	Space group	*a*(Å)	*b*(Å)	*c*(Å)	*V*(Å^3)
PrSFC	*pm-3m*	3.8563			57.3494
NdSFC	*pnma*	5.4926	7.6989	5.5684	235.467
SmSFC	*pnma*	5.4750	7.6893	5.5620	234.159
GdSFC	*pnma*	5.4649	7.6951	5.5497	233.382

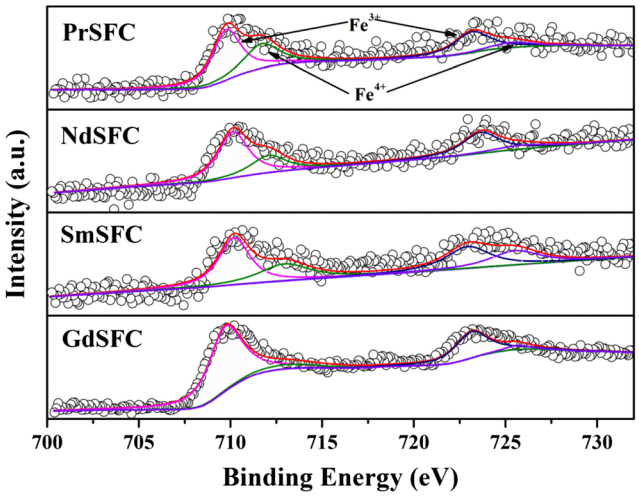

Fig. 2 Fe 2p XPS spectra of LnSFC sample

XPS analysis

The valence state of B-site metal cation for LnSFC sample was analyzed using XPS. Figures 2 and 3 show the XPS spectra of Fe 2p and Cu 2p. Table 2 lists the relative content and average valence of different valence elements. As shown in Fig. 2, the peaks of Fe $2p_{3/2}$ and $2p_{1/2}$ appeared at 709.7–710.2 eV and 722.9–723.6 eV, pointing the existence of Fe^{3+} species. The remaining peaks were observed near 711.6–713.0 eV and 725.3–725.8 eV, which were attributable to Fe^{4+} species. This value matches well with the data in some literature [30, 31]. This indicates that both Fe^{3+} and Fe^{4+} are present in the LnSFC sample. The atomic ratio of Fe^{3+}/Fe^{4+} is listed in Table 2. The atomic ratio of Fe^{3+}/Fe^{4+} in PrSFC, NdSFC, SmSFC, and GdSFC was calculated to be 68:32, 72:28, 61:39, and 89:11, respectively.

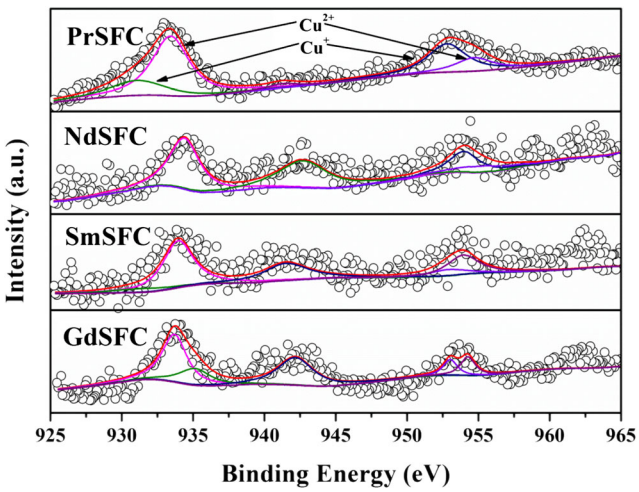

Fig. 3 Cu 2p XPS spectra of LnSFC sample

Table 2 The relative cation ratios and average valences of B-site cations for LnSFC samples

Sample	The relative cation ratios (%)				The average valences of B-site cation
	Fe^{3+}	Fe^{4+}	Cu^{+}	Cu^{2+}	
PrSFC	68	32	42	58	2.45
NdSFC	72	28	26	74	2.51
SmSFC	61	39	46	54	2.47
GdSFC	89	11	38	62	2.37

Figure 3 represents the Cu 2p XPS spectrum of the LnSFC sample. The Cu $2p_{3/2}$ and $2p_{1/2}$ peaks appeared at 932.1–933.7 eV and 952.5–952.9 eV, respectively, pointing the existence of Cu^{+} species. And the other two peaks were observed near 933.7–934.8 eV and 954.2–954.4 eV, respectively, pointing the existence of Cu^{2+} species. The peaks observed at 941.4–942.7 eV are satellite peak. This is in good agreement with some of the previous results [32, 33]. This indicates that there are two valence states of Cu^{+} and Cu^{2+} in the LnSFC sample. Table 2 shows the atomic ratio of Cu^{+}/Cu^{2+}. The atomic ratio of PrSFC, NdSFC, SmSFC, and GdSFC were calculated to be 42:58, 64:36, 46:54, and 38:62, respectively.

The average valence of the B-site metal ion is also shown in Table 2. It can be seen that the average valence of Cu and Fe cations in all samples are less than 3+. In order to maintain electrical neutrality, the oxygen vacancies can be produced with the reduction of positive charge [34]. Therefore, the Fe^{3+}/Fe^{4+} and Cu^{+}/Cu^{2+} mixed valence states of B-site cations has positive effect on the electrochemical performance of the LnSFC.

Electrical conductivity

The perovskite LnSFC cathode material is a mixed ion and electron (MIEC) conductor. The conductivity herein is mainly refers to the electronic conductivity because the electronic conductivity is several orders of magnitude higher than the ionic conductivity in MIEC oxides. Figure 4 shows the relationship between the conductivity of the LnSFC sample and the test temperature. As the temperature increases, the conductivity of the sample begins to increase, exhibiting a semiconductor-like behavior. The maximum values of conductivity appear at 300~450 °C. After the temperature exceeds 450 °C, the conductivity decreases and exhibits a similar metal conduction behavior. This phenomenon has also been found in previous studies [25, 35]. The reduction of the B-site cations (Fe and Cu) accompanied by the formation of oxygen vacancies results in a decrease in the conductivity of the LnSFC at elevated temperatures. As shown in Fig. 4, in LnSFC samples, the conductivity of PrSFC is the highest at all the temperatures tested. Over the entire temperature range, as the ionic radius decreases from Pr to Gd, the conductivity decreases monotonously. Lee et al. observed similar relationship for $Ln_{0.6}Sr_{0.4}CoO_{3-\delta}$ (Ln = La, Pr, Nd, Sm, and Gd) [36]. They investigated that the reason of these observations may be due to an increase of oxygen vacancy concentration with the decrease of Ln^{3+} ionic radius from Ln = Pr to Gd. Currently, at operating temperatures, conductivity greater than 100 S cm^{-1} is a significant symbol for fuel cell cathode materials, ensuring that sufficient current is collected [26]. Nevertheless, it has been reported that several perovskite cathode materials have

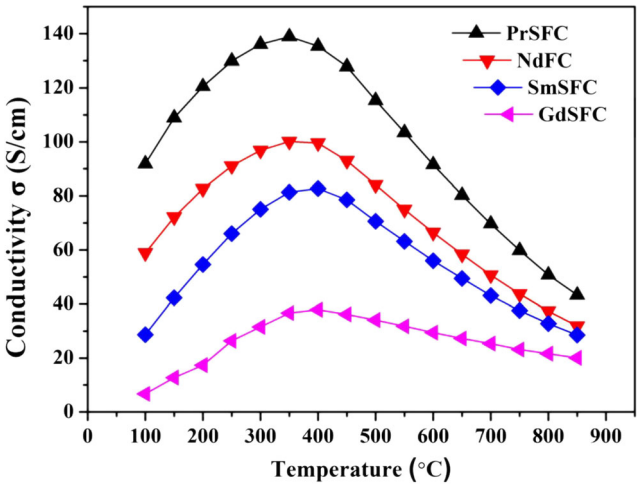

Fig. 4 The temperature dependence of electrical conductivity for LnSFC samples

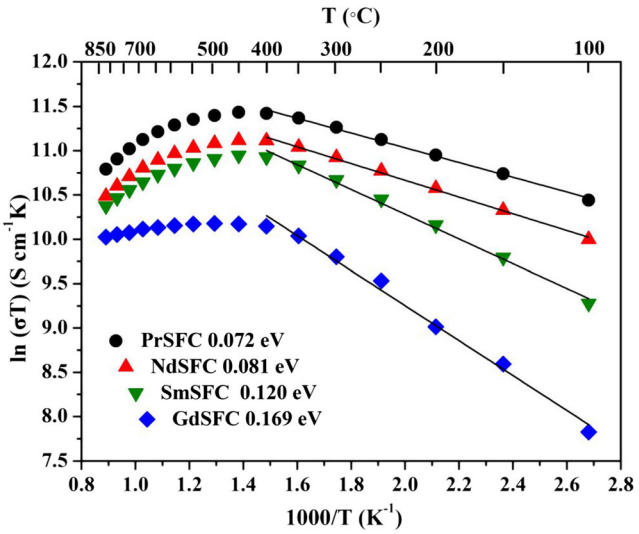

Fig. 5 The Arrhenius plots of conductivity for LnSFC in the air

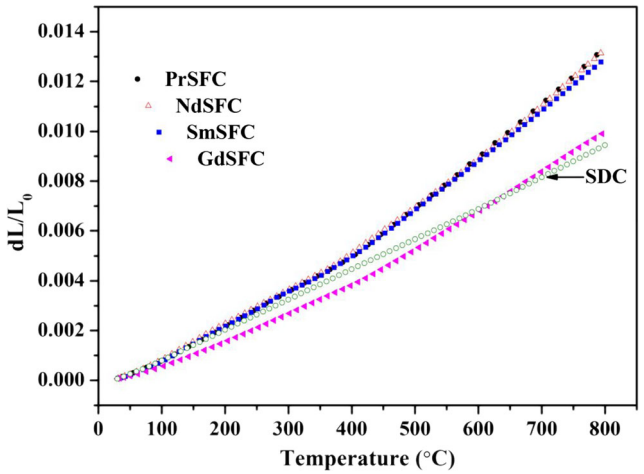

Fig. 6 Thermal expansion curves of the LnSFC samples

relatively low electrical conductivity and good electrochemical properties. For example, Zhao et al. reported that the maximum conductivity of $Ba_{0.5}Sr_{0.5}Co_{0.8}Fe_{0.2}O_{3-\delta}$ was 45 S cm^{-1} at 550 °C [37]. The conductivity of $Cu_{1.4}Mn_{1.6}O_4$ cathode materials reached ~ 70 S cm^{-1} at 750 °C [38]. In the impedance section, we can see that LnSFC sample shows a better electrochemical property.

The Arrhenius plot of conductivity for LnSFC oxides is shown in Fig. 5. At lower temperatures (100–400 °C), the plots are nearly linear. The conductivity activation energy of the four samples can be accessed on the slope of the linear part. The calculated activation energies of the PrSFC, NdSFC, SmSFC, and GdSFC are 0.072, 0.081, 0.120, and 0.169 eV, respectively. Compared with NdSFC, SmSFC, and GdSFC, the transport of charge carriers for PrSFC is relatively easier. These values are similar in magnitude to previously reported activation energies for $La_{0.6}Sr_{0.4}Fe_{0.8}Cu_{0.2}O_{3-\delta}$ oxide [39]. Moreover, the activation energies of LnSFC are lower than other cobalt-free cathode materials such as $Sm_{1.875}Ba_{3.125}Fe_5O_{15-\delta}$ (22.4 kJ/mol) [40] and $SmBa_{0.5}Sr_{0.5}CuFeO_{5+\delta}$ (116.89 kJ/mol) [41]. This conductive behavior is consistent with small polaron hopping mechanism (i.e., localized electronic carriers having a thermally activated mobility), follows the relation:

$$\sigma = (A/T)\exp(-E_a/kT) \quad (1)$$

where A is the pre-exponential factor, E_a is the activation energy for hopping conduction, k is the Boltzmann constant, and T is the absolute temperature. The charge compensation for LnSFC is primarily electrons, and the conductivity can be attributed to the migration of electron holes. At higher temperatures, the electrical conductivity decreases with the increase of testing temperature. It is obvious that there is a significant negative deviation from linearity in the plots, indicating that this conductive behavior is not consistent with low temperature assumption. At high temperature range (400–800 °C), ionic compensation becomes significant due to the loss of the lattice oxygen and can thus be related to a decreasing concentration of electron holes as the concentration of oxygen vacancies increases in the material, as expressed in Eq. (2) [42]:

$$2B_B^{\bullet} + O_o^{x} \rightarrow V_B^{\bullet\bullet} + 2B_B^{x} + \frac{1}{2}O_2 \quad (2)$$

where "x" refers to neutrality with respect to the lattice. Therefore, electrical conductivity decreases with increasing temperature due to the partial annihilation of electron holes. Similar results have been reported in the other perovskite materials [43].

Thermal expansion

Figure 6 shows the TEC of the LnSFC samples tested from room temperature to 800 °C. And the average TEC values of the LnSFC samples are shown in Table 3. The TEC values of the PrSFC, NdSFC, SmSFC, and GdSFC are 17.30, 17.19, 16.72, and 12.89×10^{-6} K^{-1}, respectively. The averages TEC are comparable to previous reports [26, 44]. In LnSFC oxides, the TEC values decrease from Ln = Pr to Gd and the TEC value of GdSFC is very close to the extensively used SDC electrolyte (12.2 × 10^{-6} K^{-1}). As the binding energy of ions in the crystal structure increases with the decrease of ion distance, the ionicity of Ln–O bond decreases, which leads to a decrease of TEC. Similar results can be seen in $Ln_{0.4}Sr_{0.6}Co_{0.8}Fe_{0.2}O_{3-\delta}$ (Ln = La, Pr, Nd, Sm, Gd) [13] and $Ln_{0.6}Sr_{0.4}CoO_{3-\delta}$ (Ln = La, Pr, Nd, Sm, and Gd) materials [36]. Figure 6 also shows that the slope of the TEC curve increases greatly when the temperature is higher than 450 ° C. It indicates that the lattice expansion accelerates with the temperature rising due to the reduction of Cu and Fe cations and consumption of the lattice oxygen. With temperature increasing, the oxygen vacancies are formed due to loss of lattice oxygen, which in turn leads to a reducing in the strength of the B–O bond intensity and an increase in the size of the BO_6 octahedron, resulting in lattice expansion. Also, in order to examine the expansibility of the samples, high-

Table 3 TEC values of LnSFC in the range of room temperature to 800 °C

Sample	PrSFC	NdSFC	SmSFC	GdSFC
TEC	17.30 × 10^{-6} K^{-1}	17.19 × 10^{-6} K^{-1}	16.72 × 10^{-6} K^{-1}	12.89 × 10^{-6} K^{-1}

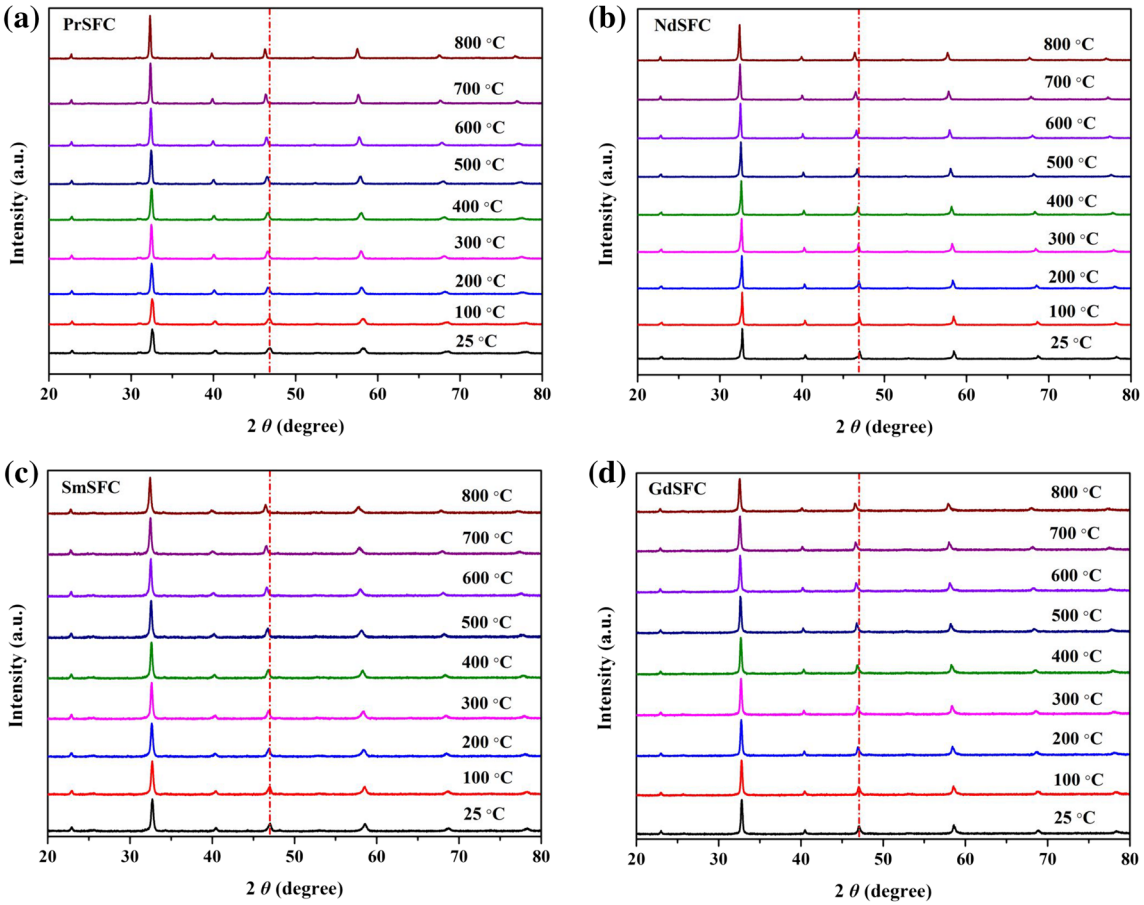

Fig. 7 High temperature powder X-ray diffraction patterns of LnSFC samples after sintering at 950 °C for 10 h **a** PrSFC, **b** NdSFC, **c** SmSFC, and **d** GdSFC

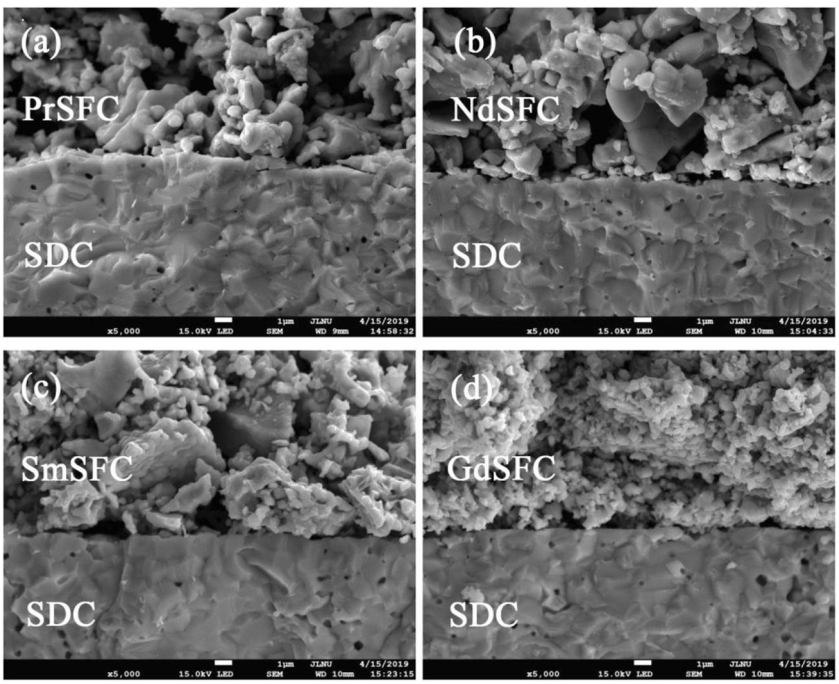

Fig. 8 Cross-section SEM micrographs of the LnSFC cathodes and SDC electrolyte

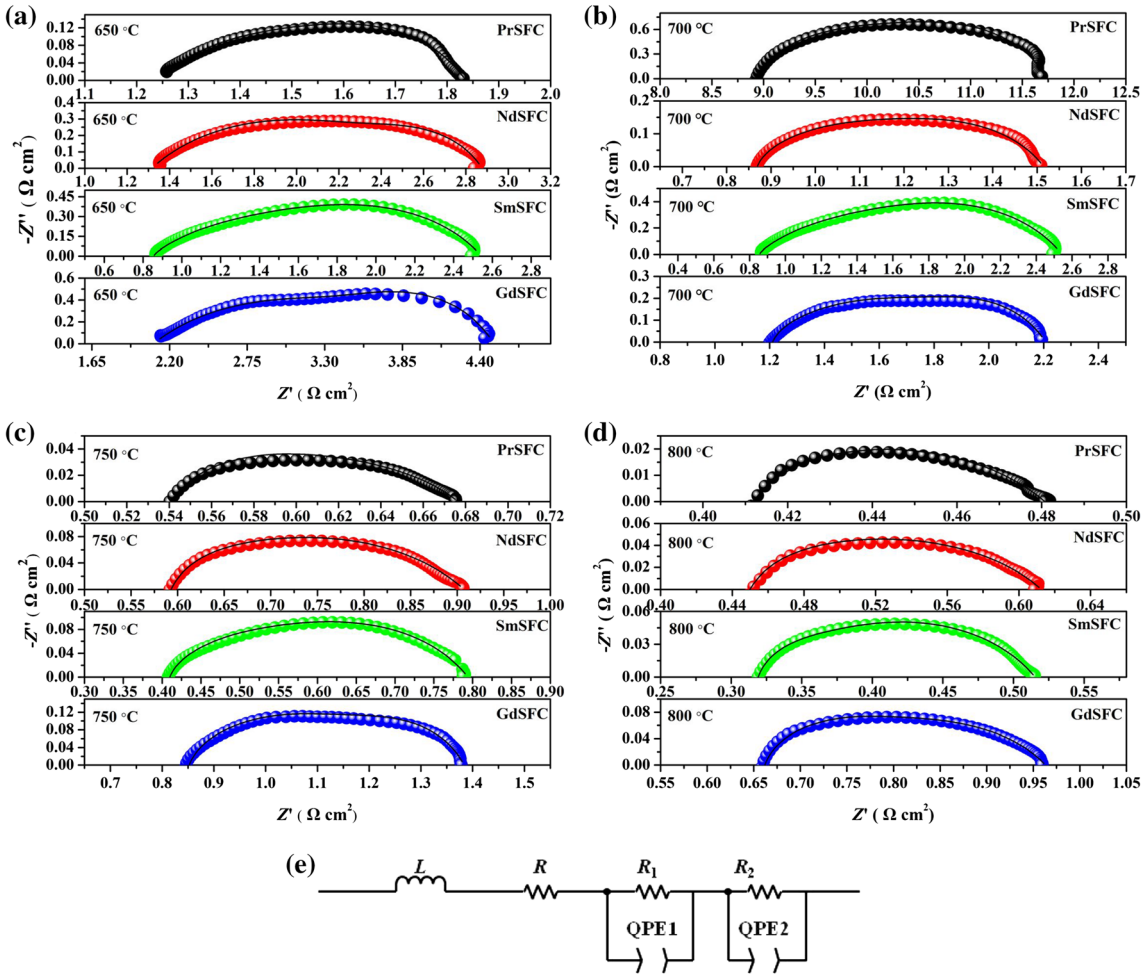

Fig. 9 Impedance spectra and equivalent circuit model of LnSFC cathode at 650 °C to 800 °C

temperature XRD (HT-XRD) measurement was conducted on the LnSFC powders after sintering at 950 °C for 10 h. The XRD patterns recorded every 100 °C are shown in Fig. 7. With increasing temperature, the main XRD peaks of the LnSFC sample shift toward the low-angle direction gradually, indicating the expansion of the perovskite lattice, which is similar with the reported B-site double perovskites [45].

Microstructure

Figure 8a–d show a cross-section microstructure of LnSFC cathodes coated on an SDC electrolyte. The sintering condition is 950 °C for 2 h. As shown in Fig. 8, the cathode structure has uniform particle and porosity, which can make the transmission of oxygen and oxygen ions more rapidly. Figure 8 illustrates that the SDC electrolyte is very dense, preventing direct contact of the fuel gas with the air, put an end to an internal short circuit. The cathode and electrolyte interface is also tightly bonded, and there is no phenomenon that the cathode layer breaks or falls off at high temperatures.

Impedance analysis

Figure 9a–d show the impedance measured for LnSFC samples in air at 750 °C and 800 °C. An equivalent circuit diagram after impedance fitting is given in Fig. 9e. *R* is an ohmic

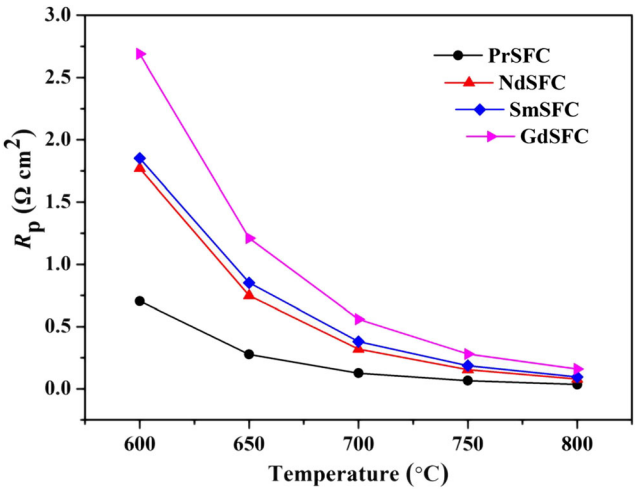

Fig. 10 The R_p of different LnSFC cathodes measured at 600–800 °C

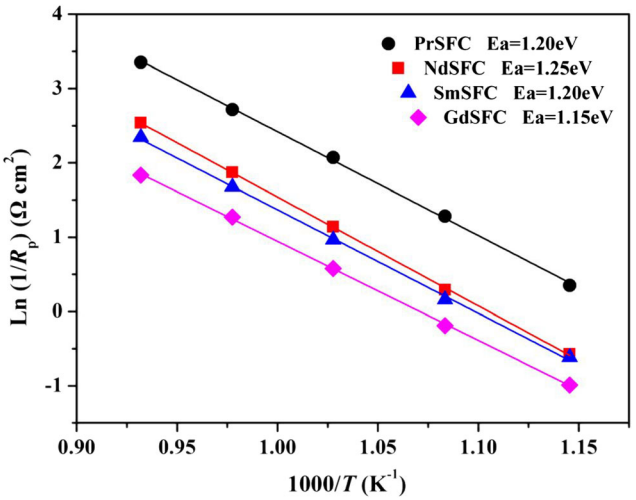

Fig. 11 Arrhenius plot of the R_p values for LnSFC cathode

resistor caused by wires and electrolytes. R_1 corresponds to the polarization resistance generated by the oxygen ion migration and diffusion process of LnSFC at high frequencies. R_2 corresponds to adsorption/dissociation during molecular oxygen, surface oxygen, or bulk oxygen diffusion at low frequencies. The sum of R_1 and R_2 is the polarization resistance (R_p) [46–48]. QPE1 and QPE2 are the capacitances of the entire electrode. As the temperature increased, the polarization resistance is reduced. The results show that the test temperature has a great influence on the electrochemical catalytic activity. The catalytic performance of the cathode is dissatisfactory at low temperatures, because the low temperature is not conducive to the migration of oxygen ions. As the temperature rises, it is easier to overcome the corresponding activation energy barrier, and the catalytic activity of the cathode is significantly improved, which promotes the reaction of the electrode, so the polarization resistance decreases with increasing temperature.

Figure 10 shows the R_p values in the range of 600 to 800 °C. The R_p of PrSFC, NdSFC, SmSFC, and GdSFC is 0.036, 0.089, 0.097, and 0.160 Ω cm^2 at 800 °C, respectively. At 750 °C, the R_p of PrSFC, NdSFC, SmSFC, and GdSFC are 0.068, 0.152, 0.190, and 0.280 Ω cm^2, respectively. It is shown that R_p of LnSFC cathode decreases with the ionic radius of the lanthanide increases. The reason of this trend may be that the surface exchange and diffusion coefficient of oxygen in the perovskite materials decreases with the decrease of rare earth ion radius, leading to an increase in R_p [49]. In previous studies [50, 51], the perovskite cathodes containing Pr ions have unusually rapid oxygen transport kinetics. In our study, in LnSFC samples, the PrSFC cathode has a lower area-specific resistance, which may be due to the change in the Pr^{3+}/Pr^{4+} valence state [32, 51]. Also, the electronic transmission capability of the PrSFC is also higher (see "XPS analysis"), which is another reason for the better electrochemical performance of the PrSFC. Moreover, the R_p of PrSFC is also related with the microstructure of electrodes. The porous

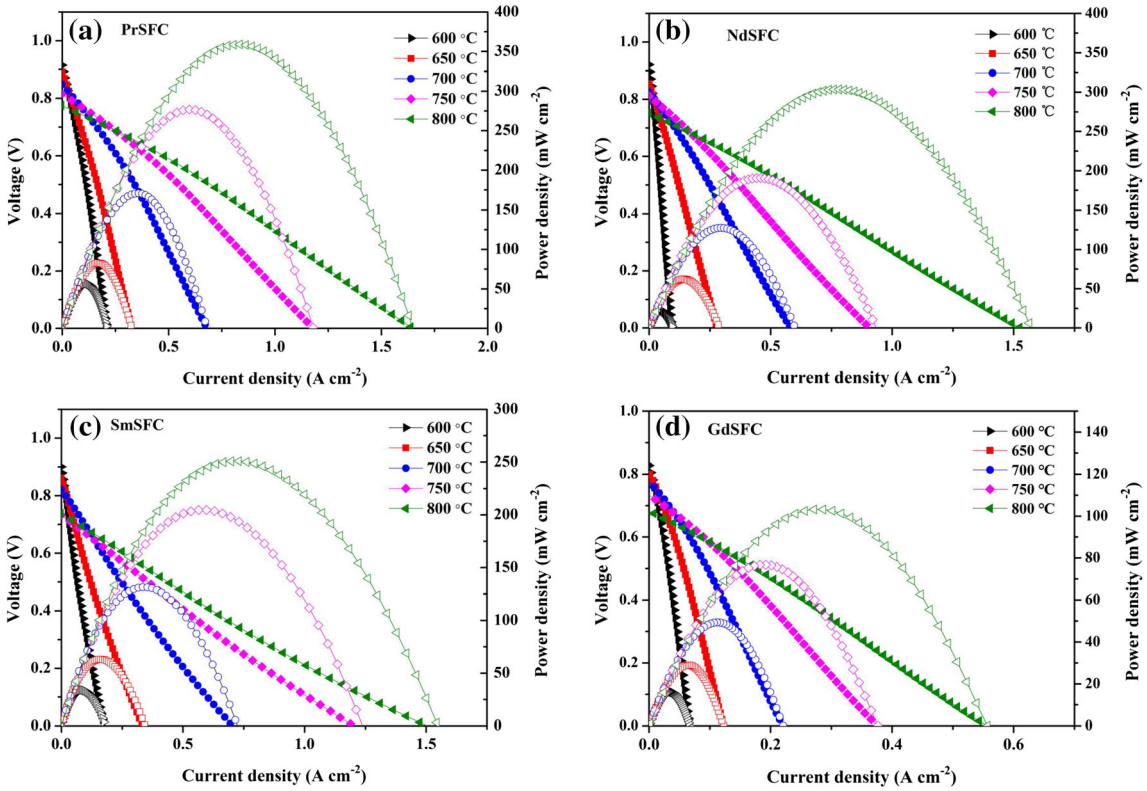

Fig. 12 Voltage and power density plots of single cell at different temperature for LnSFC cathode **a** PrSFC, **b** NdSFC, **c**, SmSFC and **d** GdSFC

microstructure will not only provide sufficient three-phase boundaries (TPB) for adsorption and diffusion of fuels, but also ensure efficient charge transfer from electrode to electrolyte or from electrolyte to electrode. In LnSFC, the GdSFC cathode has the highest polarization resistance, but the R_P values are also smaller than other Co-free cathodes such as $La_{0.7}Sr_{0.3}CuO_{3-\delta}$ (0.234 Ω cm^2 at 800 °C) [52] and $Nd_{1.6}Sr_{0.4}NiO_4$ (0.93 Ω cm^2 at 700 °C) [53]. The Arrhenius plot of the R_p for the LnSFC is displayed in Fig. 11. The calculated activation energy was 1.20, 1.25, 1.20, and 1.15 eV for PrSFC, NdSFC, SmSFC, and GdSFC, respectively. It is much smaller than 1.26 eV of the cobalt-free $Ba_{0.95}Ca_{0.05}FeO_{3-\delta}$ cathode [54].

Single-cell performance

Figure 12 shows *I*–*V* curves of an SDC electrolyte-supporting single cell using cobalt-free LnSFC as cathodes. As the temperature rises, power density of single cell gradually increases. However, the open-circuit voltage of cells is still lower than theoretical value, which is mainly caused by the reduction of Ce^{4+} to Ce^{3+} at the anode atmosphere. When the temperature is 800 °C, the peak power densities of PrSFC, NdSFC, SmSFC, and GdSFC cathodes are 364, 311, 254, and 103 mW cm^{-2}, respectively. When the temperature is 700 °C, the maximum power densities of PrSFC, NdSFC, SmSFC, and GdSFC is 280, 212, 205, and 76 mW cm^{-2}, respectively. Compared with other three samples, PrSFC obtained the best cell performance, which is consisted with the results of conductivity and polarization impedance. Moreover, the single cell with LnSFC cathodes get better power density compared with some cobalt-free cathode materials. For example, the peak power density of $Pr_{1.95}Ce_{0.05}CuO_4$ cathode based on electrolyte-supported fuel cell is 150 mW cm^{-2} 800 °C [55]. The initial finding suggests that Co-free LnSFC perovskite oxide is a potential cathode for IT-SOFC. In addition, a higher cell performance can be achieved through optimizing the cathode structure and using anode-supported single cells.

Conclusions

The cobalt-free LnSFC perovskite was successfully synthesized as a cathode for IT-SOFC. The LnSFC cathode materials exhibit structural change with increasing radius size of the lanthanide ions from cubic (Ln = PrSFC) to orthorhombic (Ln = NdSFC, SmSFC, and GdSFC) perovskite. The LnSFC material has good chemical compatibility with the SDC electrolyte. At 800 °C, the R_p values of PrSFC, NdSFC, SmSFC, and GdSFC are 0.036, 0.089, 0.097, and 0.160 Ω cm^2, respectively. The peak power densities of an electrolyte-supported single cell with PrSFC, NdSFC, SmSFC, and GdSFC as cathodes are 363.8, 311.3, 253.6, and 103.2 mW cm^{-2}, respectively. The results show that the fuel cell using LnSFC cathode has good electrochemical performance. Preliminary results indicate that the LnSFC material can be applied as a potential cathode for SOFC.

Funding information This work was supported by the Natural Science Foundation of China (nos. 51902126, 61605059 and 21701047), Program for the development of Science and Technology of Jilin province (nos. 20180414008GH and 20180520191JH), the 13th Five-Year Program for Science and Technology of Education Department of Jilin Province (nos. JJKH20180784KJ and JJKH20191024KJ), Open Project of Key Laboratory of Functional Materials Physics and Chemistry of the Ministry of Education, Jilin Normal University (no. 2016002) and Program for the development of Science and Technology of Siping City (no. 2017055).

References

1. Baharuddin NA, Muchtar A, Somalu MR (2017) Short review on cobalt-free cathodes for solid oxide fuel cells. Int J Hydrog Energy 42:9149–9155. https://doi.org/10.1016/j.ijhydene.2016.04.097
2. Hossain S, Abdalla AM, Jamain SNB, Zaini JH, Azad AK (2017) A review on proton conducting electrolytes for clean energy and intermediate temperature-solid oxide fuel cells. Renew Sust Energ Rev 79:750–764. https://doi.org/10.1016/j.rser.2017.05.147
3. Ramadhani F, Hussain MA, Mokhlis H, Hajimolana S (2017) Optimization strategies for solid oxide fuel cell (SOFC) application: a literature survey. Renew Sust Energ Rev 76:460–484. https://doi.org/10.1016/j.rser.2017.03.052
4. Meng G, Ma G, Ma Q, Peng R, Liu X (2007) Ceramic membrane fuel cells based on solid proton electrolytes. Solid State Ionics 178: 697–703. https://doi.org/10.1016/j.ssi.2007.02.018
5. Shin JF, Xu W, Zanella M, Dawson K, Savvin SN, Claridge JB, Rosseinsky MJ (2017) Self-assembled dynamic perovskite composite cathodes for intermediate temperature solid oxide fuel cells. Nat Energy 2:16214. https://doi.org/10.1038/nenergy.2016.214
6. Jiang S, Zhou W, Sunarso J, Ran R, Shao Z (2015) A cobalt-free layered oxide as an oxygen reduction catalyst for intermediate-temperature solid oxide fuel cells. Int J Hydrog Energy 40: 15578–15584. https://doi.org/10.1016/j.ijhydene.2015.09.097
7. Brett DJ, Atkinson A, Brandon NP, Skinner SJ (2008) Intermediate temperature solid oxide fuel cells. Chem Soc Rev 37:1568–1578. https://doi.org/10.1039/B612060C
8. Heremans JJ, Carris M, Watts S, Yu X, Dahmen KH, von Molnár S (1997) Characterization of films of $La_{1-x}Sr_xMnO_{3-\delta}$ grown by means of metal organic chemical vapor deposition. J Appl Phys 81:4967–4969. https://doi.org/10.1063/1.365014
9. Co AC, Xia SJ, Birss VI (2005) A kinetic study of the oxygen reduction reaction at $LaSrMnO_3$-YSZ composite electrodes. J Electrochem Soc 152:A570–A576. https://doi.org/10.1149/1.1859612
10. Kim C, Park H, Jang I, Kim S, Kim K, Yoon H, Paik U (2018) Morphologically well-defined $Gd_{0.1}Ce_{0.9}O_{1.95}$ embedded $Ba_{0.5}Sr_{0.5}Co_{0.8}Fe_{0.2}O_{3-\delta}$ nanofiber with an enhanced triple phase boundary as cathode for low-temperature solid oxide fuel cells. J Power Sources 378:404–411. https://doi.org/10.1016/j.jpowsour.2017.12.065
11. Zhou W, Ran R, Shao Z, Jin W, Xu N (2008) Evaluation of A-site cation-deficient $(Ba_{0.5}Sr_{0.5})_{1-x}Co_{0.8}Fe_{0.2}O_{3-\delta}$ (x>0) perovskite as a solid-oxide fuel cell cathode. J Power Sources 182:24–31. https://doi.org/10.1016/j.jpowsour.2008.04.012

12. Świerczek K (2011) Physico-chemical properties of $Ln_{0.5}A_{0.5}Co_{0.5}Fe_{0.5}O_{3-\delta}$ (Ln: La, Sm; A: Sr, Ba) cathode materials and their performance in electrolyte-supported intermediate temperature solid oxide fuel cell. J Power Sources 196:7110–7116. https://doi.org/10.1016/j.jpowsour.2010.08.063
13. Tu HY, Takeda Y, Imanishi N, Yamamoto O (1999) $Ln_{0.4}Sr_{0.6}Co_{0.8}Fe_{0.2}O_{3-\delta}$ (Ln=La, Pr, Nd, Sm, Gd) for the electrode in solid oxide fuel cells. Solid State Ionics 117:277–281. https://doi.org/10.1016/S0167-2738(98)00428-7
14. Chaianansutcharit S, Hosoi K, Hyodo J, Ju YW, Ishihara T (2015) Ruddlesden popper oxides of $LnSr_3Fe_3O_{10-\delta}$ (Ln = La, Pr, Nd, Sm, Eu, and Gd) as active cathodes for low temperature solid oxide fuel cells. J Mater Chem A 3:12357–12366. https://doi.org/10.1039/c5ta01273b
15. Piao J, Sun K, Zhang N, Chen X, Xu S, Zhou D (2007) Preparation and characterization of $Pr_{1-x}Sr_xFeO_3$ cathode material for intermediate temperature solid oxide fuel cells. J Power Sources 172:633–640. https://doi.org/10.1016/j.jpowsour.2007.05.023
16. Huang S, Wang G, Sun X et al (2012) Cobalt-free perovskite $Ba_{0.5}Sr_{0.5}Fe_{0.9}Nb_{0.1}O_{3-\delta}$ as a cathode material for intermediate temperature solid oxide fuel cells[J]. J Alloys Compd 543:26–30. https://doi.org/10.1016/j.jallcom.2012.07.115
17. Vázquez S, Basbus J, Soldati AL, Napolitano F, Serquis A, Suescun L (2015) Effect of the symmetric cell preparation temperature on the activity of $Ba_{0.5}Sr_{0.5}Fe_{0.8}Cu_{0.2}O_{3-\delta}$ as cathode for intermediate temperature Solid Oxide Fuel Cells. J Power Sources 274:318–323. https://doi.org/10.1016/j.jpowsour.2014.10.064
18. Long W, Xu H, He T (2014) Preparation and electrochemical performance of cobalt-free cathode material $Ba_{0.5}Sr_{0.5}Fe_{0.9}Nb_{0.1}O_{3-\delta}$ for intermediate-temperature solid oxide fuel cells. Chem Res Chinese U 30:806–810. https://doi.org/10.1007/s40242-014-4130-y
19. Gao L, Zhu M, Li Q, Sun L, Zhao H, Grenier J-C (2017) Electrode properties of Cu-doped $Bi_{0.5}Sr_{0.5}FeO_{3-\delta}$ cobalt-free perovskite as cathode for intermediate-temperature solid oxide fuel cells. J Alloys Compd 700:29–36. https://doi.org/10.1016/j.jallcom.2017.01.026
20. Gong Z, Hou J, Wang Z, Cao J, Zhang J, Liu W (2015) A new cobalt-free composite cathode $Pr_{0.6}Sr_{0.4}Cu_{0.2}Fe_{0.8}O_{3-\delta}$-$Ce_{0.8}Sm_{0.2}O_{2-\delta}$ for proton-conducting solid oxide fuel cells. Electrochim Acta 178:60–64. https://doi.org/10.1016/j.electacta.2015.07.159
21. Zhu M, Cai Z, Xia T, Li Q, Huo L, Zhao H (2016) Cobalt-free perovskite $BaFe_{0.85}Cu_{0.15}O_{3-\delta}$ cathode material for intermediate-temperature solid oxide fuel cells. Int J Hydrog Energy 41:4784–4791. https://doi.org/10.1016/j.ijhydene.2016.01.071
22. Lim YH, Lee J, Yoon JS, Kim CE, Hwang HJ (2007) Electrochemical performance of $Ba_{0.5}Sr_{0.5}Co_xFe_{1-x}O_{3-\delta}$ (x=0.2–0.8) cathode on a ScSZ electrolyte for intermediate temperature SOFCs. J Power Sources 171:79–85. https://doi.org/10.1016/j.jpowsour.2007.05.050
23. Cong L, He T, Ji Y, Guan P, Huang Y, Su W (2003) Synthesis and characterization of IT-electrolyte with perovskite structure $La_{0.8}Sr_{0.2}Ga_{0.85}Mg_{0.15}O_{3-\delta}$ by glycine–nitrate combustion method. J Alloys Compd 348:325–331. https://doi.org/10.1016/S0925-8388(02)00859-9
24. Ling Y, Yu J, Lin B, Zhang X, Zhao L, Liu X (2011) A cobalt-free $Sm_{0.5}Sr_{0.5}Fe_{0.8}Cu_{0.2}O_{3-\delta}$–$Ce_{0.8}Sm_{0.2}O_{2-\delta}$ composite cathode for proton-conducting solid oxide fuel cells. J Power Sources 196:2631–2634. https://doi.org/10.1016/j.jpowsour.2010.11.017
25. Shahgaldi S, Yaakob Z, Khadem DJ, Ahmadrezaei M, Daud WRW (2011) Synthesis and characterization of cobalt-free $Ba_{0.5}Sr_{0.5}Fe_{0.8}Cu_{0.2}O_{3-\delta}$ perovskite oxide cathode nanofibers. J Alloys Compd 509:9005–9009. https://doi.org/10.1016/j.jallcom.2011.06.117
26. Lu J, Yin Y-M, Ma Z-F (2013) Preparation and characterization of new cobalt-free cathode $Pr_{0.5}Sr_{0.5}Fe_{0.8}Cu_{0.2}O_{3-\delta}$ for IT-SOFC. Int J Hydrog Energy 38:10527–10533. https://doi.org/10.1016/j.ijhydene.2013.05.164
27. Wang J, Saccoccio M, Chen D, Gao Y, Chen C, Ciucci F (2015) The effect of A-site and B-site substitution on $BaFeO_{3-\delta}$: an investigation as a cathode material for intermediate-temperature solid oxide fuel cells. J Power Sources 297:511–518. https://doi.org/10.1016/j.jpowsour.2015.08.016
28. Zheng K, Klimkowicz A, Świerczek K, Malik A, Ariga Y, Tominaga T, Takasaki A (2015) Chemical diffusion and surface exchange in selected Ln–Ba–Sr–Co–Fe perovskite-type oxides. J Alloys Compd 645:S357–S360. https://doi.org/10.1016/j.jallcom.2014.12.110
29. Xu Q, D-p H, Chen W, Zhang F, Wang B-t (2007) Structure, electrical conducting and thermal expansion properties of $Ln_{0.6}Sr_{0.4}Co_{0.2}Fe_{0.8}O_3$ (Ln=La, Pr, Nd, Sm) perovskite-type complex oxides. J Alloys Compd 429:34–39. https://doi.org/10.1016/j.jallcom.2006.04.005
30. Jin F, Shen Y, Wang R, He T (2013) Double-perovskite $PrBaCo_{2/3}Fe_{2/3}Cu_{2/3}O_{5+\delta}$ as cathode material for intermediate-temperature solid-oxide fuel cells. J Power Sources 234:244–251. https://doi.org/10.1016/j.jpowsour.2013.01.172
31. Ghaffari M, Shannon M, Hui H, Tan OK, Irannejad A (2012) Preparation, surface state and band structure studies of $SrTi_{(1-x)}Fe_{(x)}O_{(3-\delta)}$ (x=0–1) perovskite-type nano structure by X-ray and ultraviolet photoelectron spectroscopy. Surf Sci 606:670–677. https://doi.org/10.1016/j.susc.2011.12.013
32. Meng X, Lü S, Yu WW, Ji Y, Sui Y, Wei M (2018) Layered perovskite $LnBa_{0.5}Sr_{0.5}Cu_2O_{5+\delta}$ (Ln = Pr and Nd) as cobalt-free cathode materials for solid oxide fuel cells. Int J Hydrog Energy 43:4458–4470. https://doi.org/10.1016/j.ijhydene.2018.01.033
33. Liu Y-X, Wang S-F, Hsu Y-F, Kai H-W, Jasinski P (2018) Characteristics of $LaCo_{0.4}Ni_{0.6-x}Cu_xO_{3-\delta}$ ceramics as a cathode material for intermediate-temperature solid oxide fuel cells. J Eur Ceram Soc 38:1654–1662. https://doi.org/10.1016/j.jeurceramsoc.2017.11.019
34. Xing GZ, Yi JB, Wang DD, Liao L, Yu T, Shen ZX, Huan CHA, Sum TC, Ding J, Wu T (2009) Strong correlation between ferromagnetism and oxygen deficiency in Cr-doped $In_2O_{3-\delta}$ nanostructures. Phys Rev B 79:174406. https://doi.org/10.1103/PhysRevB.79.174406
35. Tai LW, Nasrallah MM, Anderson HU, Sparlin DM, Sehlin SR (1995) Structure and electrical-properties of $La_{1-x}Sr_xCo_{1-y}Fe_yO_3$. Part 1.The system $La_{0.8}Sr_{0.2}Co_{1-y}Fe_yO_3$. Solid State Ionics 76:259–271. https://doi.org/10.1016/0167-2738(94)00244-M
36. Lee KT, Manthiram A (2006) Comparison of $Ln_{0.6}Sr_{0.4}CoO_{3-\delta}$ (Ln=La, Pr, Nd, Sm, and Gd) as cathode materials for intermediate temperature solid oxide fuel cells. J Electrochem Soc 153:A794–A798. https://doi.org/10.1149/1.2172572
37. Zhao H, Shen W, Zhu Z, Li X, Wang Z (2008) Preparation and properties of $Ba_xSr_{1-x}Co_yFe_{1-y}O_{3-\delta}$ cathode material for intermediate temperature solid oxide fuel cells. J Power Sources 182:503–509. https://doi.org/10.1016/j.jpowsour.2008.04.046
38. Zhen S, Sun W, Li P, Tang G, Rooney D, Sun K, Ma X (2016) High performance cobalt-free $Cu_{1.4}Mn_{1.6}O_4$ spinel oxide as an intermediate temperature solid oxide fuel cell cathode. J Power Sources 315:140–144. https://doi.org/10.1016/j.jpowsour.2016.03.046
39. Zhou QJ, Xu L, Guo YJ, Jia D, Li Y, Wei WCJ (2012) $La_{0.6}Sr_{0.4}Fe_{0.8}Cu_{0.2}O_{3-\delta}$ perovskite oxide as cathode for IT-SOFC. Int J Hydrogen Energy 37:11963–11968. https://doi.org/10.1016/j.ijhydene.2012.05.114
40. Zhou Q, Chen L, Cheng Y, Xie Y (2016) Cobalt-free quintuple perovskite $Sm_{1.875}Ba_{3.125}Fe_5O_{15-\delta}$ as a novel cathode for intermediate temperature solid oxide fuel cells. Ceram Int 42:10469–10471. https://doi.org/10.1016/j.ceramint.2016.03.174
41. Ding X, Kong X, Wu H, Zhu Y, Tang J, Zhong Y (2012) $SmBa_{0.5}Sr_{0.5}Cu_2O_{5+\delta}$ and $SmBa_{0.5}Sr_{0.5}CuFeO_{5+\delta}$ layered

perovskite oxides as cathodes for IT-SOFCs. Int J Hydrog Energy 37:2546–2551. https://doi.org/10.1016/j.ijhydene.2011.10.080

42. Stevenson JW, Armstrong TR, Pederson LR et al (1996) Electrochemical properties of mixed conducting $La_{1-x}M_xCo_{1-y}Fe_yO_{3-\delta}$ (M = Sr, Ca, Ba) perovskites. J Electrochem Soc 9: 2722–2729. https://doi.org/10.1149/1.1837098
43. Zhao C, Zhou QJ, Zhang T, Qu LW, Yang X, Wei T (2019) Preparation and electrochemical properties of $La_{1.5}Pr_{0.5}NiO_4$ and $La_{1.5}Pr_{0.5}Ni_{0.9}Cu_{0.1}O_4$ cathode materials for intermediate-temperature solid oxide fuel cells. Mater Res Bull 113:25–30. https://doi.org/10.1016/j.materresbull.2019.01.016
44. Lu J, Yin Y-M, Yin J, Li J, Zhao J, Ma Z-F (2015) Role of Cu and Sr in improving the electrochemical performance of cobalt-free $Pr_{1-x}Sr_xFe_{1-y}Cu_yO_{3-\delta}$ cathode for intermediate temperature solid oxide fuel cells. J Electrochem Soc 163:F44–F53. https://doi.org/10.1149/2.0181602jes
45. Du Z, Zhao H, Li S et al (2018) Exceptionally high performance anode material based on lattice structure decorated double perovskite $Sr_2FeMo_{2/3}Mg_{1/3}O_{6-\delta}$ for solid oxide fuel cells. Adv Energy Mater 2018:1800062. https://doi.org/10.1002/aenm.201800062
46. Adler S, Chen X, Wilson J (2007) Mechanisms and rate laws for oxygen exchange on mixed-conducting oxide surfaces. J Catal 245: 91–109. https://doi.org/10.1016/j.jcat.2006.09.019
47. Fu C, Sun K, Zhang N, Chen X, Zhou D (2007) Electrochemical characteristics of LSCF–SDC composite cathode for intermediate temperature SOFC. Electrochim Acta 52:4589–4594. https://doi.org/10.1016/j.electacta.2007.01.001
48. Wang Y, Zhao X, Lü S, Meng X, Zhang Y, Yu B, Li X, Sui Y, Yang J, Fu C, Ji Y (2014) Synthesis and characterization of $SmSrCo_{2-x}Mn_xO_{5+\delta}$ (x=0.0, 0.2, 0.4, 0.6, 0.8, 1.0) cathode materials for intermediate-temperature solid-oxide fuel cells. Ceram Int 40: 11343–11350. https://doi.org/10.1016/j.ceramint.2014.03.113
49. Kim JH, Manthiram A (2008) $LnBaCo_2O_{5+\delta}$ oxides as cathodes for intermediate-temperature solid oxide fuel cells. J Electrochem Soc 155:B385–B390. https://doi.org/10.1149/1.2839028
50. Jin F, Xu H, Long W, Shen Y, He T (2013) Characterization and evaluation of double perovskites $LnBaCoFeO_{5+\delta}$ (Ln = Pr and Nd) as intermediate-temperature solid oxide fuel cell cathodes. J Power Sources 243:10–18. https://doi.org/10.1016/j.jpowsour.2013.05.187
51. Ishihara T, Kudo T, Matsuda H, Takita Y (1995) Doped $PrMnO_3$ perovskite oxide as a new cathode of solid oxide fuel cells for low temperature operation. J Electrochem Soc 142:1519–1524. https://doi.org/10.1149/1.2048606
52. Ding X, Kong X, Jiang J, Cui C, Guo L (2010) Electrochemical performance of $La_{0.7}Sr_{0.3}CuO_{3-\delta}$-$Sm_{0.2}Ce_{0.8}O_{2-\delta}$ functional graded composite cathode for intermediate temperature solid oxide fuel cells. Int J Hydrog Energy 35:1742–1748. https://doi.org/10.1016/j.ijhydene.2009.12.025
53. Sun L-P, Li Q, Zhao H, Huo L-H, Grenier J-C (2008) Preparation and electrochemical properties of Sr-doped Nd_2NiO_4 cathode materials for intermediate-temperature solid oxide fuel cells. J Power Sources 183:43–48. https://doi.org/10.1016/j.jpowsour.2008.05.001
54. Wang J, Lam KY, Saccoccio M, Gao Y, Chen D, Ciucci F (2016) Ca and In Co-doped $BaFeO_{3-\delta}$ as a cobalt-free cathode material for intermediate-temperature solid oxide fuel cells. J Power Sources 324:224–232. https://doi.org/10.1016/j.jpowsour.2016.05.089
55. Kolchina LM, Lyskov NV, Kuznetsov AN, Kazakov SM, Galin MZ, Meledin A, Abakumov AM, Bredikhin SI, Mazo GN, Antipov EV (2016) Evaluation of Ce-doped Pr_2CuO_4 for potential application as a cathode material for solid oxide fuel cells. RSC Adv 6:101029–101037. https://doi.org/10.1039/C6RA21970E